

Orientation effects in the fusion of $^{28}\text{Si}+^{28}\text{Si}$ system using SEDF

Atul Choudhary* and Dalip Singh Verma†

*Department of Physics and Astronomical Science,
Central University of Himachal Pradesh, Dharamshala,
District Kangra,(H.P)-176215, INDIA*

Introduction

The study of orientation effects is significant as it gives the most favourable configuration for the nuclei to fuse. For this, we have extended the semiclassical extended Thomas-Fermi approach of Skyrme energy density formalism (SEDF) for deformed and oriented nuclei, although quadrupole deformation only. The orientation and deformations dependence in SEDF is included through the nuclear density. Here, two parameter Fermi density is used as nuclear density and is extended to deformed nuclei by using deformed nuclear radius and surface diffuseness of ref. [1]. These parameters for spherical nuclei are taken from the earlier work of one of us [2]. The nuclear proximity potential is obtained in slab approximation and overlap of density distribution is considered in sudden approximation. The total interaction potential is obtained by adding deformed Coulomb and centrifugal terms explicitly to the proximity part. We fixed the orientation of the one of the interacting nucleus and varied the orientation of the other in steps of 15° so as to obtain the maximum barrier height and the minimum interaction radius, a configuration favoured for hot fusion [3]. The characteristic properties of the total interaction potential obtained for this configuration is used in Hill-Wheeler approximation, an alternate to the one dimensional solution to the Schrödinger wave equation with appropriate boundary conditions, for a given partial wave. The transmission probability is obtained in parabolic approximation and the total fusion cross-section is calculated by adding partial waves up to certain maximum value ℓ_{max} .

For comparing our results, we have chosen $^{28}\text{Si}+^{28}\text{Si}$ system for which fusion evaporation residues were measured in a recent experiment [4] over center of mass-energy (E_{cm}) range $\simeq 31-39$ MeV and coupled channel (CC) calculations were implemented to reproduce the observed fusion data. In an another experiment [5] of same group

(a year ago) over $E_{cm} \simeq 22 - 30$ MeV, the CC calculations were done by adjusting the parameters of the interaction potential. Similarly, for some other older experiments [6–8] over E_{cm} range ($\simeq 30 - 220$ MeV), Esbensen, et al. [9] has calibrated the potential parameters within the CC calculation. Now, with these above mentioned experiments the fusion cross-section data for $^{28}\text{Si}+^{28}\text{Si}$ system is available for over a wide range of energy both well below and quite above the barrier but there is no unique choice of interaction potential available in literature for the calculations of fusion cross-section. So, here we have achieved suitable interaction potential for the fusion process by varying nuclear orientations.

Methodology

The nuclear potential, $V_N(R)$ in semiclassical extended Thomas-Fermi approach of SEDF using slab approximation (see Ref. [2]) is,

$$V_N(R) = 2\pi\bar{R} \int_{s_0}^{\infty} \left[H(\rho, \tau, \vec{J}) - \sum_{i=1}^2 H_i(\rho_i, \tau_i, \vec{J}_i) \right] dz$$

where \bar{R} is the mean curvature radius for deformed nuclei, $H(\rho, \tau, \vec{J})$ is Skyrme Hamiltonian density and $\rho(= \sum_i \rho_i)$, $\tau(= \sum_i \tau_i)$, $\vec{J}(= \sum_i \vec{J}_i)$, are nuclear, kinetic energy and spin-orbit densities respectively for composite system, $i = 1, 2$ for the two interacting nuclei. The two parameter Fermi density distribution in slab approximation for axially symmetric deformed and oriented nuclei is

$$\rho_i(z_i, \alpha_i, T) = \rho_{0i}(T) \left[1 + \exp\left(\frac{z_i - R_i(\alpha_i, T)}{a_i(\alpha_i, T)}\right) \right]^{-1} \quad (1)$$

where $R_i(\alpha_i, T)$ and $a_i(\alpha_i, T)$ are nuclear radii and surface diffuseness parameters for deformed, oriented and coplanar nuclei of [1], respectively. The angle α_i is the angle between nuclear symmetry axis and radius vector, and are uniquely defined for each nuclei after satisfying the minimisation condition [3] for the separation between the interacting surfaces, for a fixed orientation. The nuclear radii and surface diffuseness parameters $R_{0i}(T)$ and $a_{i0}(T)$ are taken from the earlier work of one of us

*Present address: G.C. Banjar, Kullu (H.P.)-175123

†Electronic address: dsverma@cuhimachal.ac.in

[2] and $\lambda(=2)$ for axially symmetric quadrupole deformation. The total interaction potential $V_T(R)$ is obtained by adding Coulomb $V_C(R)$ and centrifugal terms $V_\ell(R)(= \hbar^2\ell(\ell+1)/2\mu R^2)$ to nuclear proximity $V_N(R)$. The characteristic properties of this potential is used in Hill-Wheeler approximation [10] to calculate the fusion cross-section, as

$$\sigma_{HW} = \frac{\pi\hbar^2}{2\mu E_{cm}} \sum_{\ell=0}^{\ell_{max}} (2\ell+1) \frac{e^{-x}}{1+e^{-x}} \quad (2)$$

where $x = 2\pi\{V_B(\ell) - E_{cm}\}/\hbar\omega_\ell$, $V_{B\ell}$ is barrier height, $R_{B\ell}$ is barrier position and μ is the reduced mass of interacting nuclei and $\ell_{max} = 38\hbar$ [9].

Calculations and results

The total interaction potential is obtained by taking various orientation of target and projectile at $\ell = 0$. The orientations of projectile and tar-

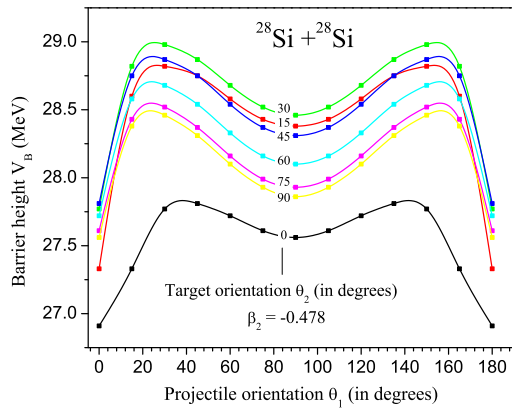


FIG. 1: The interaction potential barrier V_B as a function projectile orientation angle θ_1 at different target orientations angle θ_2 .

get are varied in steps of 15° to obtained an orientation which gives maximum barrier height at $\ell = 0$. Fig. 1 shows this variation of V_B with projectile orientation θ_1 for fixed orientation of target θ_2 , at different target orientations θ_2 . This figure clearly shows that the V_B first increase, become maximum and then decreases when $\theta_1 \rightarrow 90^\circ$. Out of all possible orientations, the orientation $(\theta_1, \theta_2) = (30^\circ, 30^\circ)$ gives maximum V_B and minimum value of R_B , a favourable configuration for the fusion reaction. This is also clear from the Table I, where the orientation effect on other potential characteristics $(V_B, R_B, \hbar\omega_0)$ is given. The characteristic properties of the potential for $(30^\circ, 30^\circ)$ configuration are used to calculate fusion cross-section with HW approximation and partial waves are considered up to $38\hbar$ as per ref. [9]. Fig. 2, shows the

Orientations: (θ_1, θ_2)	V_B (MeV)	R_B (fm)	$\hbar\omega_0$ (MeV)
Spherical	28.23	9.05	2.87
$(0^\circ, 30^\circ), (180^\circ, 30^\circ)$	27.77	9.14	2.90
$(15^\circ, 30^\circ), (165^\circ, 30^\circ)$	28.82	8.76	2.85
$(30^\circ, 30^\circ), (150^\circ, 30^\circ)$	28.98	8.73	2.81
$(45^\circ, 30^\circ), (135^\circ, 30^\circ)$	28.87	8.81	2.78
$(60^\circ, 30^\circ), (120^\circ, 30^\circ)$	28.68	8.90	2.75
$(75^\circ, 30^\circ), (105^\circ, 30^\circ)$	28.52	8.98	2.75
$(90^\circ, 30^\circ), (90^\circ, 30^\circ)$	28.46	9.01	2.72

TABLE I: The characteristic properties of the total interaction potential for various orientations of projectile at fixed target $\theta_2 = 30^\circ$ for $\ell = 0$.

calculated fusion excitation function for $^{28}\text{Si}+^{28}\text{Si}$ system over $E_{cm} \simeq 22 - 229$ MeV at $(30^\circ, 30^\circ)$ orientation and is compared with the observed data [4–8]. It clear from the figure that $(30^\circ, 30^\circ)$ config-

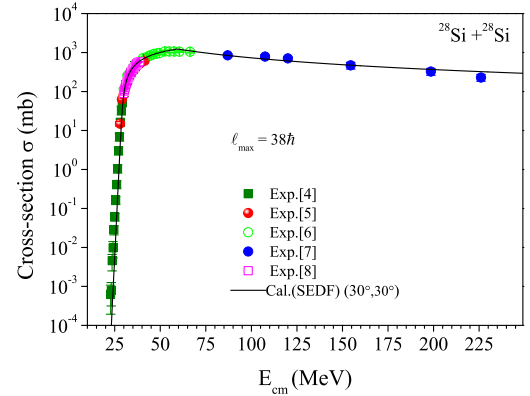


FIG. 2: Fusion excitation function for $^{28}\text{Si}+^{28}\text{Si}$ system for most favour configuration for hot fusion compared with experimental data [4–8] over a wide E_{cm} range.

uration is the favoured configuration for the fusion process and the number of partial waves required to be included is $38\hbar$.

References

- [1] A. Bohr, B. R. Mottelson, Nuclear Structure: Vol II: Nuclear Deformations, World Scientific (1998).
- [2] R. K. Gupta, D. Singh *et al.*, J. Phy. G: Nucl. Part. Phys **36**, 075104 (2009).
- [3] R. K. Gupta, N. Singh *et al.*, Phys. Rev. C **70**, 034608 (2004).
- [4] G. Montagnoli, *et al.*, Phys. Lett. B **746**, 300(2015).
- [5] G. Montagnoli, *et al.*, Phys. Rev. C **90**, 44608(2014)
- [6] M.F. Vineyard *et al.*, Phys. Rev. C **41**, 1005 (1990).
- [7] Y. Nagashima *et al.*, Phys. Rev. C **33**, 176 (1986).
- [8] S. Gary & C. Volant, Phys. Rev. C **25**, 1877 (1982).
- [9] H. Esbensen, Phys. Rev. C **85**, 064611 (2012).
- [10] D. L. Hill, J. A. Wheeler, Phys. Rev. **89**, 1102 (1953).